Iraqi Journal of Natural Sciences and Nanotechnology IJNSN

Structural and Optical Evolution of SnO_2 Thin Films with Precursor Concentration Variation via Thermochemical Decomposition

Qutoof Shihab Shukr[1*], Mahir N. Thameel[1], J. F. Mohammad[1]

Department of Physics, College of Education for Pure Science, University Of Anbar, Anbar, Ramadi, Iraq

Corresponding Author : qat22u3015@uoanbar.edu.iq

Keywords:

SnO_2 Thin Films; Thermochemical Decomposition; Precursor Concentration; Optical Properties; Surface Morphology

Abstract

This paper presents a study on the synthesis of nanostructured tin dioxide (SnO_2) thin films via thermochemical decomposition of $SnCl_2.2H_2O$ (0.01 M, 0.02 M, and 0.03 M). The systematic influence of precursor concentration on morphological and optical properties of the films was studied by a combination of scanning electron microscopy (SEM), atomic force microscopy (AFM), and UV-Vis spectroscopy. SEM and AFM studies confirmed that with the increase in concentration, there is a gradual increment in grain size and surface roughness. The grain size mean was changed by increasing the average grain size overall 29.81 nm to 51.84 nm and the mean surface roughness varied between 24.70 nm and 43.38 nm. Optical absorption measurements showed that it is strongly absorbed in the UV region with absorption coefficients greater than 10^4 cm^{-1}. Analysis of Tauc plots indicates a direct allowed transition where the optical bandgap decreased systematically as quantum confinement descended and crystallinity increased (3.80 eV, 0.01 M to 3.68 eV, 0.03 M). There was further enhancement in refractive index at a higher concentration indicating enhanced film density and compactness in the structure. These findings demonstrate that the precursor concentration is a central factor in controlling the structure and optical properties of SnO_2 thin films and a scalable approach to material optimization in optoelectronic, sensing, and energy devices.

Introduction

Tin dioxide (SnO_2), a wide-bandgap semiconductor (Eg ≈ 3.6-4.0 eV), is extensively exploited in transparent conducting oxides (TCOs), UV photodetectors, gas sensors, and energy devices, where the high optical transparency, chemical stability, and electron mobility are important [1, 2]. The optical and structural properties of SnO_2 films are strongly induced by synthesis parameters, particularly precursor concentration [3]. Numerous of searches have presented that loading more of Sn precursor will increases the crystallinity and reduces the band gap. Hassan et al. (2019) additionally highlighted that the precursor concentration does not only affect the film morphology but also the electronic behavior, as demonstrated that higher $SnCl_2$

concentration shifted the preferred crystal orientations and also affected the current-voltage response in SnO_2/Si heterojunctions [4].
The precursor concentration has also been associated with alterations in the nucleation kinetics and agglomeration of grains that lead to the modulation of film microstructure and light absorption. The positive response of photocatalytic activity and conductivity to increasing concentrations of precursors in the experimental work of Enesca and Du (2010) was attributed to the ability of material in high concentrations to enhance the granular growth and inter-grain connectivity [5]. Izydorczyk et al. (2014) also noted that spinning films with a higher concentration of Sn precursor results in more compact grain packaging and higher optical density [6]. Further observations by Farva and Kim (2021) indicated that whilst their study was conducted to investigate the effect of deposition temperature, the interaction between precursor dissociation and thin-film structure indicated a bandgap reduced and better carrier concentration and carrier mobility were obtained upon optimal growth conditions, which is in line with findings under elevated precursor concentration conditions [7]. To corroborate this, Kim et al. (2021) stressed that in sol-gel-derived SnO2 thin-film transistors, thicker and smoother thin-film transistors were observed upon enhancement of the precursor concentration, which ultimately raised the charge mobility and low threshold voltages [8].
Recent studies proved that the concentration of precursor is an important factor that can affect the nanostructural growth of SnO_2 thin films in a significant way. Chatterjee and Kar (2021) observed that morphological transitions of ZnO nanospheres to nanosheets, a red shift in absorption edge, and photoluminescence response are evident by increasing zinc nitrate precursor concentration in thin films, with clear dependencies between precursor concentration, defects in the crystal, and optical properties [9]. This concentration-dependent modulation was also seen in SnO2 systems. Roza and Rahman (2024) discovered that increasing the concentration of SnCl2.2H2O in Al-doped SnO2 films led to an increase in grain development, photoluminescence output, and transparency, which demonstrated greater crystallinity and a low defect level [10]. In analogous fashion, Laghrib et al. (2023) observed that at higher precursor molarity in indium-doped SnO2 films resulted in enhanced grain uniformity and transmittance, and lowered the bandgap- desirable in UV optoelectronics [11]. This trend is supported by Sharma et al. (2024) who demonstrated that structural optimization of compositional control in SnO2 thin films improved optical absorption and carrier mobility, vital parameters in device performances [12]. Lastly, Ye et al. (2021) noted that flexibility and crystallinity, which are closely related to precursor concentration, significantly influence the optical and electronic characteristics of SnO2-based flexible UV photodetectors [13].

Although many reports exist on the effect of precursor concentration on SnO_2 thin films prepared via sol-gel, spray-pyrolysis, and spin-coating, very little exists in combination of thermochemical decomposition using fixed low deposition temperature (= 350 °C) and a systematic multi-technique characterization - that is, coupling of AFM-derived nanoscale roughness and topography with SEM-observed grain morphology with UV-Vis-derived optical constants. Such a procedure allows the direct structure-property connection, which is frequently ignored in precursor concentration experiments. Moreover, through the use of three distinct molarities (0.01 M, 0.02 M, 0.03 M) at the same temperature, the current work isolates precursor concentration as a single processing parameter, disentangling the similarity of temperature or doping. The findings offer a common understanding covering the surface morphology, crystallinity and optical performance, which can serve as practical guidelines to optimize the SnO_2 films in the context of the optoelectronics and sensing applications that involve extensive transparency and desired surface topography.

Materials and Methods

Materials

Tin(II) chloride dihydrate ($SnCl_2 \cdot 2H_2O$, molecular weight: 225.63 g/mol) was employed as the precursor for SnO_2 thin film synthesis. This reagent, supplied by Oxford Lab Chem (India), is a white crystalline powder with a purity of 99.98% and high solubility in ethanol. Absolute ethanol (purity 99.5%) was used as the solvent. Microscope glass slides (dimensions: 25 mm × 25 mm) served as substrates. Prior to deposition, all substrates were subjected to a sequential ultrasonic cleaning process using acetone, ethanol, and deionized

water for 10 minutes each, followed by drying at ambient temperature to ensure surface cleanliness and enhance film adhesion.

Thin Film Preparation

SnO_2 precursor solutions with concentrations of 0.01 M, 0.02 M, and 0.03 M were prepared by dissolving appropriate amounts of $SnCl_2 \cdot 2H_2O$ in absolute ethanol under continuous magnetic stirring at room temperature for 1 hour to ensure complete dissolution and homogeneity. All solutions were freshly prepared prior to deposition to minimize hydrolysis and maintain solution stability. The deposition was carried out via the chemical thermal decomposition (CTD) method. Cleaned glass substrates were heated and maintained at a fixed surface temperature of 350 °C. The precursor solution was sprayed onto the heated substrates using a fine atomizing nozzle positioned 25 cm above the surface, with a constant spray rate of 1.5 mL/min. The thermal energy of the substrate induced in-situ decomposition of the precursor, leading to the direct formation of SnO_2 thin films without the need for additional post-annealing. After deposition, the samples were allowed to cool naturally to room temperature. The resulting films exhibited high optical transparency, strong adhesion to the substrates, and uniform surface coverage, with estimated thicknesses ranging from 200 nm to 300 nm depending on precursor concentration.

Surface Morphology Analysis

Surface topography was studied using Atomic Force Microscopy (AFM), model JPK NanoWizard II from Bruker (Germany), operating in tapping mode over a $0.49 \times 0.49\ \mu m^2$ scan area. Surface morphology and particle distribution also examined by Scanning Electron Microscopy (SEM) using a TESCAN MIRA 3 instrument, manufactured in the Czech Republic. SEM imaging was conducted at high magnification (100,000×).

Optical transmittance and absorption spectra were recorded using a PerkinElmer UV–Vis Double Beam Spectrophotometer in the wavelength range of 300–800 nm. Absorbance (A), transmittance (T%), the absorption coefficient (α), and the optical band gap energy (energy difference, E_g) were obtained and calculated using Tauc relation based on the absorbances and transmittances, respectively. In addition, the refractive index (n) and the extinction coefficient (k) were determined using a set of equations that relied on the laws of Fresnel and the dispersion theory.

The absorption coefficient (α) was calculated using [14]:

$$\alpha = \frac{2.303\,A}{t} \qquad (1)$$

Where A is the absorbance, t is the film thickness (in cm), α is the absorption coefficient (cm^{-1}). The optical band gap (Eg) was determined from Tauc's relation [15]:

$$(\alpha h\nu)^m = B_o\left(h\nu - E_g\right) \qquad (2)$$

Where hν is the photon energy (eV), Bo is a constant, m denotes the type of optical transition (m = ½ for direct allowed transitions, m = 2 for indirect allowed transitions). The extinction coefficient (k) was calculated using [16]:

$$k = \frac{\lambda\alpha}{4\pi} \qquad (3)$$

The refractive index (n) was calculated using reflectance data (R) and the extinction coefficient (k) [13]:

$$n = \left\{\left[\left(\frac{1+R}{1-R}\right)^2 - k^2\right]^{1/2} + \left(\frac{1+R}{1-R}\right)\right\} \qquad (4)$$

Results and discussion

SEM analysis results

SEM images in Figure (1) revealed notable morphological changes with increasing precursor concentration. At 0.01 M Figure 1(a), films revealed reasonably dense, spherical grains with partial voids and an average size of ~44 nm, representing partial nucleation The existence of intergranular voids means that the surface is not fully covered and this can affect the optical transmittance and porosity of the film [18]. At 0.02 M Figure (b), the surface developed more uniformity with smaller grains (~37 nm) and improved coverage, exhibiting higher nucleation density and film homogeneity. The reduction in the mean grain size explained by a higher nucleation density, which imposed by an increased supply of tin ions in the solution and inhibits the growth of the individual grains [19, 20]. At 0.03 M Figure (c), a high compact was observed in the structure of grain coalescence and negligible porosity; grain size slightly improved (~38 nm) with visible aggregation. These developments approve that higher precursor concentrations result in denser, less porous films by increased tin ion accessibility and grain impingement [21].

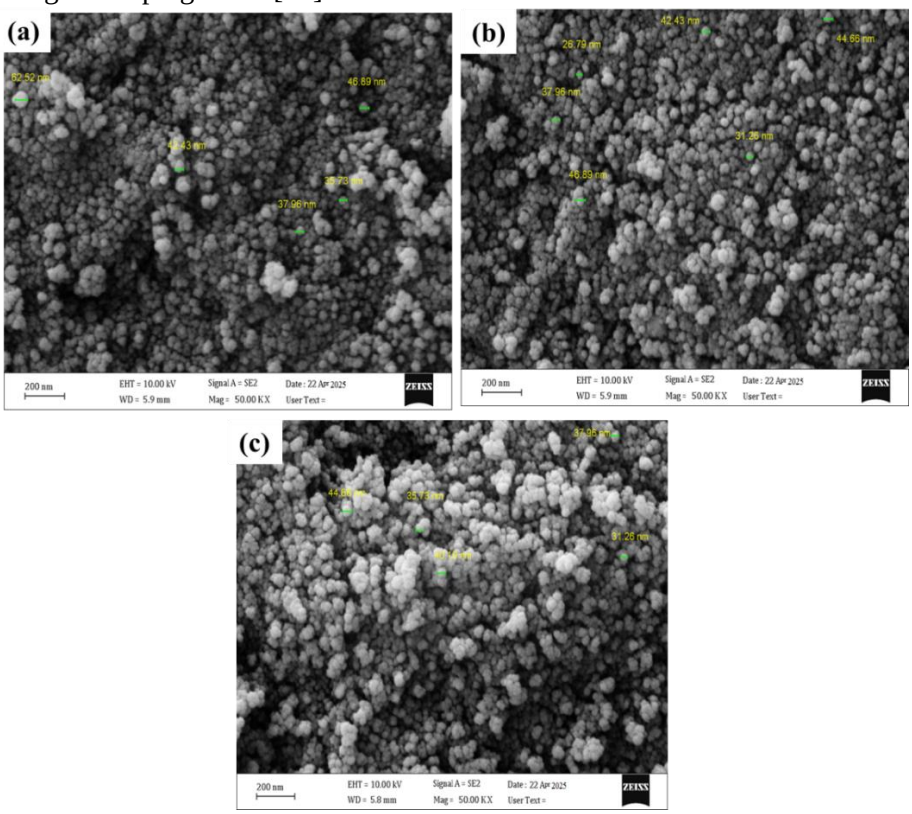

Figure 1 SEM surface morphology images of SnO_2 thin films deposited at 350 °C using precursor concentrations of 0.01 M (a), 0.02 M (b), and 0.03 M (c).

Table 1 shows a clear comparison between the data constructed from SEM measurements for the three concentrations of precursor. Als, it presents a comparative analysis of the grain size and topography of the SnO_2 thin films prepared at various concentrations of the precursors.

Table 1 Comparative Summary of SEM Analysis

Precursor Concentration	Grain Size Range (nm)	Average Grain Size (nm)	Surface Morphology	Notable Features
0.01 M	35.73 – 62.52	~44	Moderately dense, smooth	Larger grains, partial voids
0.02 M	26.79 – 46.89	~37	Denser, uniform	Finer grains, tightly packed, good coverage
0.03 M	31.26 – 44.66	~38	Very compact, aggregated	Coalesced grains, minimal porosity

AFM analysis results

AFM results in Figure 2(a–c) and Table 2 reveal a consistent increase in surface roughness and grain size with rising precursor concentration, directly linking nanoscale morphology to potential performance differences between pristine and interaction-enhanced films. At 0.01 M (Figure 2(a)), the average grain size was 29.81 nm and the mean surface roughness (Ra) was 24.70 nm, indicating a smooth, uniform surface with moderate protrusions. The nanoscale homogeneity across the scan area suggests favorable deposition conditions for uniform film formation. This relatively low roughness promotes high optical transparency and minimal scattering, which is desirable in applications such as transparent conductive oxides (TCOs). However, the limited surface area may restrict activity in applications that require high interfacial reactivity, such as gas sensing or photocatalysis [22]. At 0.02 M (Figure 2(b)), Ra increased to 33.89 nm and grain size to 33.19 nm. The denser texture and higher grain density indicate enhanced nucleation and surface texturing. This intermediate surface heterogeneity increases the available surface area-to-volume ratio, beneficial for surface-dependent applications such as photoelectrochemical energy conversion and catalytic reactions, while still retaining acceptable optical transparency [23, 24]. At 0.03 M (Figure 2(c)), both Ra and grain size reached their maximum values (43.38 nm and 51.84 nm, respectively), accompanied by a maximum height of 255 nm. This morphology corresponds to a precursor-rich growth regime favoring rapid surface diffusion, vertical stacking, and grain aggregation. Such compact, vertically textured surfaces significantly enhance light–surface interaction, optical absorption, and gas adsorption potential. However, the clustered grain structure may also introduce localized stress and defect states, which must be considered in device stability assessments [25].
The systematic trend—smooth and modest-density morphologies at low concentrations (0.01 M) transitioning to rough, compact, and vertically textured surfaces at higher concentrations (0.03 M)—is consistent with the grain coarsening observed in SEM (Figure 1) and the crystallinity enhancements revealed by XRD (Figure 3). This cross-validation between techniques removes interpretation conflicts and confirms that increasing precursor concentration promotes both vertical and lateral grain growth, leading to improved grain connectivity and potential functional performance.

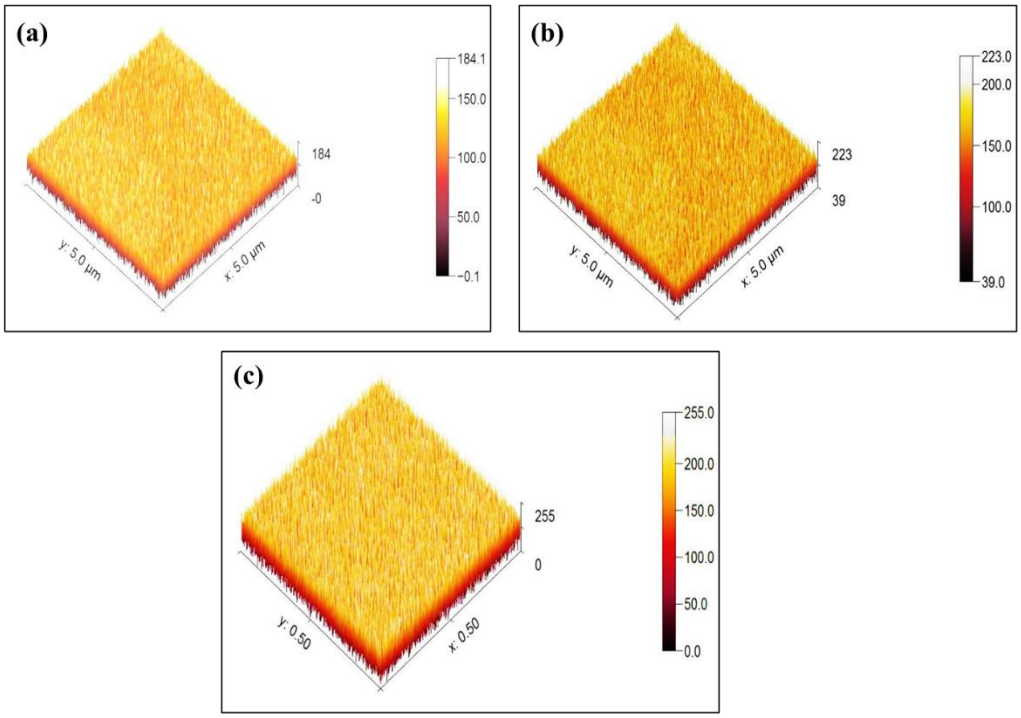

Figure 2 Three-dimensional AFM surface topography images of SnO_2 thin films deposited at 350 °C using precursor concentrations of 0.01 M (a), 0.02 M (b), and 0.03 M (c).

Table 2 Comparative Summary of AFM Topography and Grain Characteristics of SnO_2 Thin Films Synthesized at 350 °C

Precursor Concentration (M)	Average Grain Size (nm)	Maximum Height (nm)	Mean Roughness (Ra, nm)	Topographical Characteristics
0.01	29.81	184	24.70	Smooth, uniform grains with moderate protrusions
0.02	33.19	233	33.89	Dense surface texture with high grain density
0.03	51.84	255	43.38	Highly rugged with clustered grains and tall features

This composite interpretation brings together the AFM, SEM and XRD interpretations, and demonstrates cleanly how precursor concentration dictates morphological development, which subsequently determines optical transparency, surface activity, and potential application feasibility.

Optical analysis results

Absorption Coefficient Analysis

Figure 3 presents the variation of the optical absorption coefficient (α) as a function of photon energy (hν) for SnO_2 thin films synthesized at 350 °C with precursor concentrations of 0.01 M, 0.02 M, and 0.03 M. All samples presented strong absorption in the UV region with absorption coefficients more than 10^4 cm^{-1}, even at moderate film thicknesses. The 0.03 M film showed the highest absorption across the photon energy spectrum,

followed by 0.02 M and 0.01 M. This improve in optical absorption is ascribed to greater film thickness, better grain packing, and decreased voids—factors that endorse light–matter interaction. The rougher surfaces at higher concentrations more participated to light trapping through multiple scattering effects. These features are vital for solar energy conversion applications
and photodetectors [2].

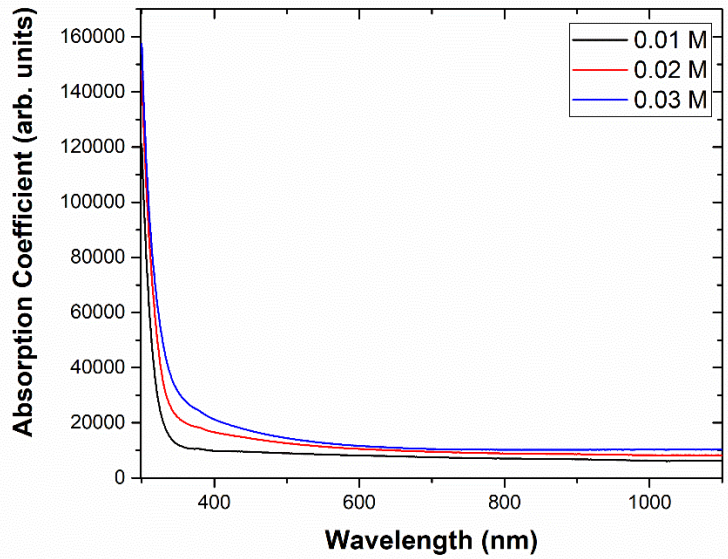

Figure 3 Optical absorption coefficient spectra of SnO_2 thin films deposited at 350 °C using precursor concentrations of 0.01 M (black), 0.02 M (red), and 0.03 M (blue).

Optical Bandgap Analysis

Figure 4 presents the Tauc plots of $(\alpha h\nu)^2$ versus photon energy ($h\nu$) for films deposited at 350 °C using precursor concentrations of 0.01 M, 0.02 M, and 0.03 M. Tauc plots verified a direct allowed transition, with decreasing the optical bandgap from 3.80 eV (0.01 M) to 3.75 eV (0.02 M) and 3.68 eV (0.03 M). The monitored redshift in Eg is a consequence of decreased quantum confinement because of larger crystallite sizes and enhanced crystallinity [26]. Furthermore, limited defects and grain boundaries at greater concentrations can further reduce the bandgap via narrowing the energy states[4]. The results that obtained from UV-vis measurements are well harmonize with the SEM and AFM data. This tunable bandgap improves the flexibility of SnO_2 films for UV photodetectors and transparent optoelectronic devices.

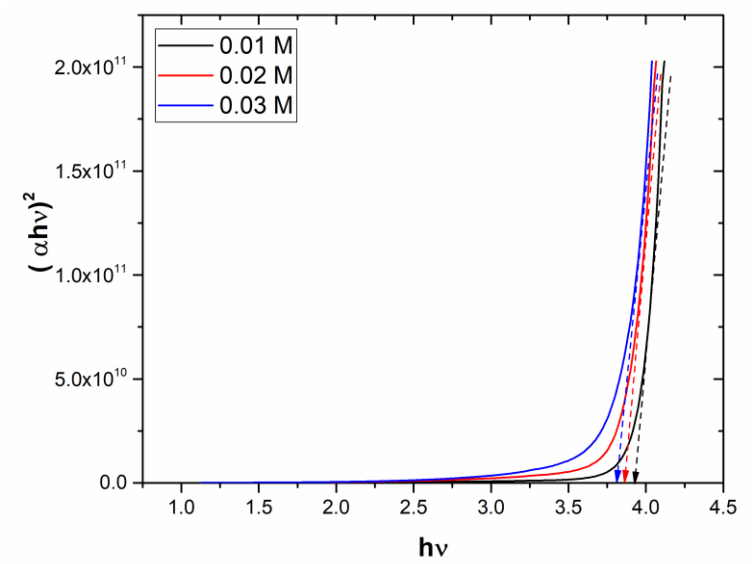

Figure 4 Tauc plots (αhν)2 versus photon energy (hν) for SnO_2 thin films deposited at 350 °C using precursor concentrations of 0.01 M (black), 0.02 M (red), and 0.03 M (blue), assuming a direct allowed electronic transition.

Refractive Index Analysis

The dispersion of the refractive index (n) of the SnO_2 thin films deposited on the substrate at 350 °C with a precursor of concentrating to 0.01 M, 0.02 M and 0.03 M is shown in Figure 5. In all of the films, the refractive index (n) is found to decrease with increasing wavelength, which is characteristic of dielectric and semiconductor materials, as the electronic polarizability decreases at lower photon energies. There is a systematic increase in n across the whole spectral range with precursor concentration, consistent with the densification tendencies effective in the SEM (Figure 1) and AFM (Figure 2) data. The lowest absorption edge in the optical spectra (Figures 3), as well as the smoother and less compact morphology at the AFM showing with Ra = 24.70 nm and grain size = 29.81 nm can be related to the lower refractive index of 0.01 M. Doubling the concentration to 0.02 M results in an increase of n, which is expected with a more packed surface and enhanced accessibility between grains, as signified by a modest roughness (Ra = 33.89 nm) and enhanced optical absorption. The 0.03 M film displays the greatest n values, suggesting the highest surface roughness (Ra = 43.38 nm) and grain size (51.84 nm), characteristic of a compact, precursor-rich growth regime leading to high film density and low porosity. These optical tendencies align with the results of the Tauc plot (Figure 4), as the film with 0.03 M concentration causes the strongest absorption onset, which means that the number of voids is minimal and the light-molecule interaction is high. The concordance between refractive index behavior and structural/morphological data strongly supports that the observed behavior of *n* increases with precursor concentration is not an arbitrary measurement artifact. The measured values of the refractive index (1.92-2.5) also agree well with literature values of nanocrystalline SnO_2 films deposited under similar conditions [27]. This tunable modification of *n* by precursor concentration offers a convenient method of adjusting SnO_2 films towards optoelectronic uses, including anti-reflective coatings, Bragg reflectors and waveguides.

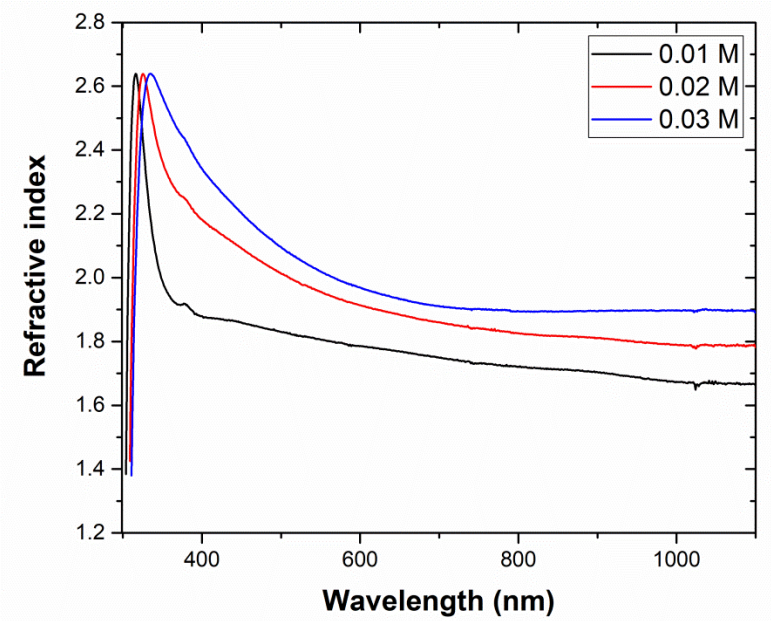

Figure 5 Refractive index dispersion as a function of wavelength for SnO_2 thin films deposited at 350 °C using precursor concentrations of 0.01 M (black), 0.02 M (red), and 0.03 M (blue).

Conclusion

SnO_2 thin films were successfully prepared via thermochemical decomposition method at 350 °C by changing precursor concentrations (0.01 M, 0.02 M, and 0.03 M) to explore their effect on morphology and optical properties. SEM and AFM studies indicated that increasing the concentration led to denser films, bigger grain size, and higher surface roughness. Optical characterization showed strong UV absorption, a redshift bandgap from 3.80 eV to 3.68 eV, and the refractive index rose in proportion with concentration of the precursor, indicative of higher film density and optical compactness. The 0.02 M film among the samples that proposed the best balance between optical performance and surface uniformity. These conclusions emphasize precursor concentration as a vital parameter for modifying SnO_2 films for optoelectronic applications.

Conflict of intterest

Authors have no conflicts of interest to declare.

References

[1] L. Fonseca, N. Oliveira, L. Martins, and L. Scalvi, "Thin film deposition of organic-inorganic quinoline-tin dioxide p-n junction for optoelectronic devices," Optical Materials: X, 2024-12-01 2024, doi: 10.1016/j.omx.2024.100361.

[2] S. Ikhmayies, "The Influence of the Substrate Temperature on the Optical Parameters of Spray-Deposited Fluorine-Doped Tin Oxide (FTO) Thin Films," JOM, 2025-01-31 2025, doi: 10.1007/s11837-025-07139-y.

[3] M. Rahman and L. Roza, "Al-doped SnO2 thin films as transparent heater: effect of tin (II) chloride concentration," Ionics, 2024-04-02 2024, doi: 10.1007/s11581-024-05479-4.

[4] A. Addie, J. Admon, and A. Hassan, "Influence of precursor concentration on the optoelectronic properties of spray deposited SnO2/Si heterojunction," Materials Research Express, vol. 6, 2019-08-02 2019, doi: 10.1088/2053-1591/ab350b.

[5] A. Enesca and A. Duţă, "The influence of the precursor concentration on the properties of SnO2 thin films," Thin Solid Films, vol. 519, pp. 568-572, 2010-11-01 2010, doi: 10.1016/J.TSF.2010.07.007.

[6] W. Izydorczyk, J. Uljanow, K. Waczyński, M. Magnuski, N. WaczyńskaNiemiec, J. Izydorczyk, J. Mazurkiewicz, P. Karasiński, and W. Filipowski, "Electrical and optical properties of spin-coated SnO2 nanofilms," Materials Science-Poland, vol. 32, pp. 729-736, 2014-12-01 2014, doi: 10.2478/s13536-014-0265-2.

[7] J. Kim and U. Farva, "Growth temperature-dependent morphological, optical, and electrical study of SnO2 thin film by atomic layer deposition," Materials Chemistry and Physics, 2021-04-10 2021, doi: 10.1016/J.MATCHEMPHYS.2021.124584.

[8] C. Lee, J. Bae, I. Kang, J. Jang, K. Kim, D. W. Kim, and H. Kim, "Influence of Active Channel Layer Thickness on SnO2 Thin-Film Transistor Performance," Electronics, 2021-01-17 2021, doi: 10.3390/ELECTRONICS10020200.

[9] S. Chatterjee and A. Kar, "Precursor concentration induced nanostructural evolution of electrodeposited ZnO thin films and its effect on their optical and photocatalytic properties," Journal of Materials Science: Materials in Electronics, vol. 33, pp. 8970-8986, 2021-10-09 2021, doi: 10.1007/s10854-021-07010-1.

[10] L. Roza and M. Rahman, "Al-doped SnO2 thin films as transparent heater: effect of tin (II) chloride concentration," Ionics, 2024-04-02 2024, doi: 10.1007/s11581-024-05479-4.

[11] S. Laghrib, M. Benhaliliba, H. Adnani, and D. Abdi, "Wide bandgap Indium-doped SnO_2 semiconductor prepared by sol-gel route: Multilayer fabrication and Low resistivity for solar cell application," Journal of Sol-Gel Science and Technology, vol. 106, pp. 530-544, 2023-04-01 2023, doi: 10.1007/s10971-023-06093-y.

[12] N. Sharma, B. Sharma, S. Das, P. Chettri, P. Karki, R. Pradhan, B. Chettri, and A. Rao, "A First-Principle Study to Investigate Electrical and Optical Properties of Tin Oxide," 2024 IEEE International Conference of Electron Devices Society Kolkata Chapter (EDKCON), pp. 573-577, 2024-11-30 2024, doi: 10.1109/EDKCON62339.2024.10870789.

[13] Q. Ye, X. Zhang, R. Yao, D. Luo, X. Liu, W. Zou, C. Guo, Z. Xu, H. Ning, and J.-B. Peng, "Research and Progress of Transparent, Flexible Tin Oxide Ultraviolet Photodetector," Crystals, 2021-11-28 2021, doi: 10.3390/cryst11121479.

[14] N. Habubi and S. Chiad, "Physical characterization of sprayed SnO2 thin films," Materials Science : an Indian Journal, vol. 10, pp. 397-401, 01/01 2014.

[15] Ł. Haryński, A. Olejnik, K. Grochowska, and K. Siuzdak, "A facile method for Tauc exponent and corresponding electronic transitions determination in semiconductors directly from UV–Vis spectroscopy data," Optical Materials, 2022-05-01 2022, doi: 10.1016/j.optmat.2022.112205.

[16] R. Martín-Palma, J. Martínez-Duart, and A. Macleod, "Determination of the optical constants of a semiconductor thin film employing the matrix method," IEEE Trans. Educ., vol. 43, pp. 63-68, 2000-02-01 2000, doi: 10.1109/13.825742.

[17] O. Urper, M. Tonka, and N. Baydogan, "Modification of optical constants at nanospherical ZnO:Al thin film," Journal of Materials Science: Materials in Electronics, vol. 34, pp. 1-11, 2023-01-25 2023, doi: 10.1007/s10854-022-09751-z.

[18] K. Juraić, P. Dubček, M. Bohač, A. Gajović, S. Bernstorff, M. Čeh, A. Hodzic, and D. Gracin, "Surface Morphology of Textured Transparent Conductive Oxide Thin Film Seen by Various Probes: Visible

Light, X-rays, Electron Scattering and Contact Probe," (in eng), Materials (Basel), vol. 15, no. 14, Jul 10 2022, doi: 10.3390/ma15144814.

[19] K. Derrar, Z. Mourad, A. Hafdallah, N. Rouabah, and B. Gasmi, "Optical and Structural Properties of SnO2 Thin Films Deposited by Spray Pyrolysis Technique: Effect of Solution Concentration," vol. 397, pp. 179-186, 09/12 2019.

[20] A. Eneşca and A. Duţă, "The influence of the precursor concentration on the properties of SnO2 thin films," Thin Solid Films, vol. 519, no. 2, pp. 568-572, 2010/11/01/ 2010, doi: https://doi.org/10.1016/j.tsf.2010.07.007.

[21] E. Leite, T. Giraldi, F. Pontes, E. Longo, A. Beltran, and J. Andres, "Crystal Growth in Colloidal Tin Oxide Nanocrystals Induced by Coalescence at Room Temperature," Appl. Phys. Lett., vol. 83, pp. 1566-1568, 08/25 2003, doi: 10.1063/1.1605241.

[22] M. Akagawa and H. Fujiwara, "Optical characterization of textured SnO2:F layers using spectroscopic ellipsometry," J. Appl. Phys., vol. 112, no. 8, 2012, doi: 10.1063/1.4759054.

[23] M. Shaban, A. Almohammedi, R. Saad, and A. M. El Sayed, "Design of SnO(2):Ni,Ir Nanoparticulate Photoelectrodes for Efficient Photoelectrochemical Water Splitting," (in eng), Nanomaterials (Basel), vol. 12, no. 3, Jan 28 2022, doi: 10.3390/nano12030453.

[24] Y. Yang, B. Maeng, D. G. Jung, J. Lee, Y. Kim, J. Kwon, H. K. An, and D. Jung, "Annealing Effects on SnO(2) Thin Film for H(2) Gas Sensing," (in eng), Nanomaterials (Basel), vol. 12, no. 18, Sep 16 2022, doi: 10.3390/nano12183227.

[25] W. Cheng, P. Huang, Z. Gao, Y. Chen, L. Ren, Q. Feng, X. Liu, S. Ahmad, and Z. Zhou, "Molecular Bridging of Buried Interface Flattens Grain Boundary Grooves and Imparts Stress Relaxation for Performance Enhancement and UV Stability in Perovskite Solar Cells," Advanced Energy Materials, vol. n/a, no. n/a, p. 2501296, doi: https://doi.org/10.1002/aenm.202501296.

[26] J. Mohamed, S. Palanichamy, L. Amalraj, K. Kumar, M. Anitha, and S. Pandiarajan, "Effect of molar concentration on physical properties of spraydeposited SnO2 thin films using nebulizer," Journal of Sol-Gel Science and Technology, vol. 89, pp. 392-402, 2018-12-01 2018, doi: 10.1007/s10971-018-4894-5.

[27] R. Outemzabet, M. Doulache, and M. Trari, "Physical and photoelectrochemical properties of Sb-doped SnO2 thin films deposited by chemical vapor deposition: application to chromate reduction under solar light," Applied Physics A, vol. 119, pp. 589-596, 2015-02-04 2015, doi: 10.1007/s00339-015-8996-4.